materials

MDPI

Article

Effects of Corrosion Products Deposited on 304 Stainless Steel on Reduction of Se (IV/VI) in Simulated Groundwater

Guokai Huang [1,†], Teng Li [2,*,†], Xian Zhang [3], Lingyu Wang [2], Daqing Cui [2,4] and Miao Yang [1,*]

[1] School of Chemistry, Chemical Engineering and Life Sciences, Wuhan University of Technology, Wuhan 430070, China; guokaihuang@whut.edu.cn
[2] Department of Radiochemistry, China Institute of Atomic Energy, Beijing 102413, China; linyuwang2955@163.com (L.W.); daqing.cui@studsvik.se (D.C.)
[3] Collaborative Innovation Center for Advanced Steels, Wuhan University of Science and Technology, Wuhan 430081, China; xianzhang@wust.edu.cn
[4] Department of Materials and Environmental Chemistry, Stockholm University, SE-106 91 Stockholm, Sweden
* Correspondence: liteng@ciae.ac.cn (T.L.); yangmiao@whut.edu.cn (M.Y.)
† These authors contributed equally to this work.

Abstract: Selenium (Se) is a key mobile fission product in the geological disposal of nuclear waste. It is necessary to analyze the reductive deposition behavior of iron-based materials to Se(IV) and Se(VI) in groundwater. In the present work, the corrosion behavior of 304 stainless steel in simulated groundwater (SG) and the effects of corrosion products on the dissolution of Se were investigated by electrochemical and immersion tests. Experimental results revealed that passivation films formed on 304 stainless-steel samples were destroyed by polarization measurements, forming corrosion products consisting of Fe(II) compounds, such as Fe_3O_4 and FeO. Corrosion products deposited on the surface of steel samples previously treated by polarization measurements in SG + $CaCl_2$/Na_2CO_3/Na_2SiO_3 solutions effectively reduced soluble Se(IV) and Se(VI) during immersion tests, depositing $FeSe_2$ on sample surfaces.

Keywords: 304 stainless steel; simulated groundwater; selenium; corrosion behavior; reduction rate

check for updates

Citation: Huang, G.; Li, T.; Zhang, X.; Wang, L.; Cui, D.; Yang, M. Effects of Corrosion Products Deposited on 304 Stainless Steel on Reduction of Se (IV/VI) in Simulated Groundwater. *Materials* **2022**, *15*, 2705. https://doi.org/10.3390/ma15082705

Academic Editor: Francesco Iacoviello

Received: 9 March 2022
Accepted: 1 April 2022
Published: 7 April 2022

Publisher's Note: MDPI stays neutral with regard to jurisdictional claims in published maps and institutional affiliations.

Copyright: © 2022 by the authors. Licensee MDPI, Basel, Switzerland. This article is an open access article distributed under the terms and conditions of the Creative Commons Attribution (CC BY) license (https://creativecommons.org/licenses/by/4.0/).

1. Introduction

Deep geological disposal is widely accepted by major nuclear power countries in the world to isolate radionuclides permanently from the biosphere [1,2]. ^{79}Se is considered a key mobile fission product for the geological disposal of nuclear waste. Selenium (Se) is a high-level radioactive waste (HLW) and exists in the form of ^{79}Se (unstable isotope) with a half-life of 3.77×10^5 years [3–5]. In the process of geological disposal of HLW, nuclides are isolated by multiple barriers; moreover, nuclides can react with corrosion products when the leakage of nuclides is caused by corrosion perforation of geological disposal containers. Therefore, the mobility of Se is a key factor for the safe disposal of HLW.

Se exists in the form of different valence compounds (−II, −I, 0, +IV, +VI) [5]. The solubility of Se is influenced by its oxidation state to some extent, and its oxidation state compounds (selenite (SeO_3^{2-}) and selenate (SeO_4^{2-})) are highly soluble under different chemical conditions, whereas Se and its selenides have very low solubility [5,6]. It has been proven that Fe(II)-containing minerals, such as green rust [7], magnetite [8–12], pyrite [13,14], and troilite [14], can reduce SeO_4^{2-} and SeO_3^{2-}, and the abiotic reduction of Fe(II)-containing minerals is very high. Se is the main reduction product of several Fe(II)-containing minerals. Iron selenide (FeSe) was found to be the main reduction product of magnetite and green rust selenite [4].

Fe(II)-containing minerals generally exist in deep geological media, and abiotic reduction has an important effect on the mobility of Se in groundwater [15]. Mingliang Kang et al. [6] investigated the interaction of aqueous Se(IV) with pyrite under O_2-free

conditions at pH ranging from 4.5 to 6.6; they found that pH and iron concentration have a significant effect on the Se(IV) reaction rate and reaction product. Mingliang Kang et al. [5] investigated the influence of pH and reaction time on the formation of $FeSe_2$ by reductive precipitation of Se(IV) with nanosized pyrite–greigite; they found that $FeSe_2$ was formed at pH > 6.07. Teng Li et al. [2] found that an Fe(II) compound-containing passivation film was formed on the surface of pure iron in simulated groundwater containing carbonate, silicate, and calcium ions.

$$Fe + 2H_2O \rightarrow Fe(OH)_2 + H_2. \quad (1)$$

$$Fe^{2+} + {CO_3}^{2-} \rightarrow FeCO_3. \quad (2)$$

$$2Fe^{2+} + {SiO_3}^{2-} + 2OH^- \rightarrow Fe_2SiO_4 + H_2O. \quad (3)$$

In order to investigate the effect of corrosion products on the migration of Se in a deep geological disposal repository after the corrosion failure of the disposal vessel, 304 stainless steel was selected as the research object to analyze the reduction adsorption and deposition behavior of Se(IV) and Se(VI) by corrosion products.

2. Experimental

2.1. Materials

Sodium chloride (NaCl; AR; Sinopharm Chemical Reagent Co. LTD.(Shanghai, China)), calcium chloride anhydrous ($CaCl_2$; AR; Sinopharm Chemical Reagent Co. LTD. (Shanghai, China)), sodium hydrogen carbonate ($NaHCO_3$; AR; Sinopharm Chemical Reagent Co. LTD. (Shanghai, China)), sodium carbonate (Na_2CO_3; AR; Sinopharm Chemical Reagent Co. LTD. (Shanghai, China)), sodium metasilicate nonahydrate ($Na_2SiO_3 \cdot 9H_2O$; AR; Sinopharm Chemical Reagent Co. LTD. (Shanghai, China)), ethanol absolute (C_2H_6O; AR; Sinopharm Chemical Reagent Co. LTD. (Shanghai, China)), sodium selenite (Na_2SeO_3; AR; Chengdu Huaxia Chemical Reagent Co. LTD. (Chengdu, China)), and sodium selenate (Na_2SeO_4; AR; Chengdu Huaxia Chemical Reagent Co. LTD. (Chengdu, China)) were the main chemicals of this experiment.

The chemical composition of the commercial 304 stainless steel used in this experiment is presented in Table 1. For the immersion test, the 304 stainless-steel plate was cut into samples of 20 mm × 10 mm × 2 mm size. Each sample was mechanically ground to 2000 grit by silicon carbide papers, washed with ethanol, and dried. For the electrochemical experiment, the 304 stainless-steel plate was cut into specimens of 10 mm × 10 mm × 2 mm size to prepare electrodes. These working electrodes were ground to 2000 grit, polished to a mirror surface, washed with ethanol, and dried.

Table 1. Chemical composition of the 304 stainless steel.

	Composition (wt.%)								
	C	**S**	**P**	**Si**	**Sn**	**Mn**	**Ni**	**Cr**	**Fe**
304 stainless steel	0.08	0.003	0.04	-	0.8	1.8	9	19	balance

2.2. Simulated Groundwater Solution

The simulated groundwater (SG) solutions used in this experiment contained SG (10 mM NaCl + 2 mM $NaHCO_3$) and different ions (Ca^{2+}, ${CO_3}^{2-}$, ${SiO_3}^{2-}$). The concentrations of Ca^{2+}, ${CO_3}^{2-}$, and ${SiO_3}^{2-}$ ions were set to 0 mM, 1 mM, 5 mM, 10 mM, or 20 mM by adding $CaCl_2$, Na_2CO_3, and Na_2SiO_3, respectively. The chemical compositions of the as-prepared simulated groundwater solutions are listed in Table 2.

2.3. Immersion Solutions

The immersion solutions used in this experiment contained SG and different valence states of Se solution (Se(IV/VI)). The concentrations of Se solution were set to 30 mg/L and

100 mg/L by adding Na_2SeO_3 or Na_2SeO_4. The chemical compositions of the as-prepared immersion solutions are listed in Table 3.

Table 2. Chemical composition of simulated groundwater.

Solution	Chemicals Concentration (mM)				
	NaCl	**$NaHCO_3$**	**$CaCl_2$**	**Na_2CO_3**	**Na_2SiO_3**
SG	10	2	0	0	0
SG + $CaCl_2$	10	2	1	0	0
	10	2	5	0	0
	10	2	10	0	0
	10	2	20	0	0
SG + Na_2CO_3	10	2	0	1	0
	10	2	0	5	0
	10	2	0	10	0
	10	2	0	20	0
SG + Na_2SiO_3	10	2	0	0	1
	10	2	0	0	5
	10	2	0	0	10
	10	2	0	0	20

Table 3. Chemical composition of the solution for the immersion test.

	Chemicals Concentration			
	NaCl	**$NaHCO_3$**	**Na_2SeO_3**	**Na_2SeO_4**
SG + Na_2SeO_3	10 mM	2 mM	30 mg/L	0
	10 mM	2 mM	100 mg/L	0
SG + Na_2SeO_4	10 mM	2 mM	0	30 mg/L
	10 mM	2 mM	0	100 mg/L

2.4. Electrochemical Measurements

In order to analyze the corrosion behavior of 304 stainless steel in anoxic SG, the potentiodynamic polarization curves of 304 stainless-steel samples at different ion concentrations were plotted by a Zahner electrochemical workstation (Germany) at 40 °C. An electrochemical cell consisting of three electrodes was used in this experiment; 304 stainless-steel samples acted as working electrodes, a saturated Hg/Hg_2Cl_2 electrode worked as the reference electrode, and a platinum foil served as the counter electrode. Each solution was purged with argon gas containing 0.03% CO_2 for 20 min to obtain a H_2- and O_2-free solution. The open-circuit potential of each solution was tested for 30 min. The potentiodynamic polarization curve of each solution was tested in a potential range of −0.3 to 1.6 V relative to the open-circuit potential. The potential sweep rate was set to 0.5 mV/s.

2.5. Immersion Test

In order to explore the corrosion behavior of 304 stainless steel, a CHI 660E electrochemical workstation was used for pitting 304 stainless steel in SG + 20 mM $CaCl_2/Na_2CO_3/Na_2SiO_3$ solutions by polarization measurements. Subsequently, the 304 stainless-steel samples treated by polarization measurements were immersed in SG solutions (Table 2) for 4 weeks. The concentrations of Se in these solutions after different immersion times were determined.

2.6. Surface Characterization

The concentrations of Se in immersion solutions were determined by an inductively coupled plasma optical emission spectrometer (ICP-OES; Prodigy 7/Prodigy 7, Hudson, NH, USA). The surface morphology and elemental composition of corrosion products

deposited on the surface of 304 stainless-steel samples after the 4 week immersion test were analyzed by a scanning electron microscope equipped with an energy-dispersive spectrometer (SEM/EDS; Zeiss Auriga FEI Quanta FEG 250 SEM/Oxford Inca X-act 2000 EDS, Hillsboro, OR, USA). The formation mechanism of corrosion products deposited on the surface of 304 stainless-steel samples after the 4 week immersion test was analyzed by a confocal Raman microscope (CRM, Renishaw, London, UK). Corrosion products deposited on the surface of 304 stainless-steel samples after the 4 week immersion test were characterized by an X-ray photoelectron spectrometer (XPS, Kratos, Manchester, UK) equipped with a monochromated Al K-α X-ray source (HV = 1486.69 eV) at 150 W.

3. Result and Discussion

3.1. Potentiodynamic Polarization Curves

The electrochemical corrosion behavior of 304 stainless steel in different SG solutions was analyzed by potentiodynamic polarization measurements at 40 °C. The polarization curves of 304 stainless steel in different SG solutions are displayed in Figure 1, and electrochemical parameters obtained from the fitted curves are listed in Table 3.

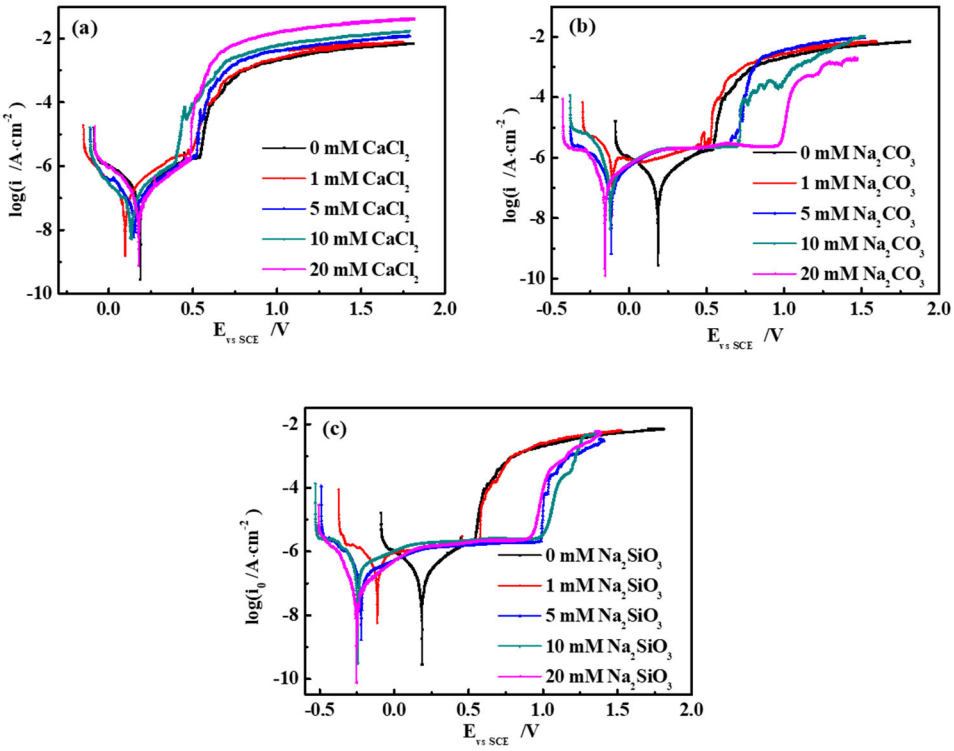

Figure 1. Polarization curves of 304 stainless steel in different simulated groundwater at 40 °C: (**a**) SG + $CaCl_2$; (**b**) SG + Na_2CO_3; (**c**) SG + Na_2SiO_3.

It is noticeable from Figure 1 that, in SG + $CaCl_2$ solutions, the polarization curves had a similar shape, indicating that the corrosion behaviors of 304 stainless-steel samples were similar under the influence of different concentrations of $CaCl_2$. The anodic polarization curve only had an activation dissolution zone. When the potential reached the pitting potential, the passivation film on the steel surface ruptured, and the corrosion current density dramatically increased. In the SG + Na_2CO_3/Na_2SiO_3 solutions, the polarization curves of 304 stainless steel had different forms. When the ion concentration was 0 mmol/L, the anodic polarization curve only had an activated dissolution zone. When the ion concentration continued to increase, the anodic polarization curve had a stable passivation zone. When the potential reached the pitting potential (Epp), the passivation film on the steel surface ruptured, and the corrosion current density dramatically increased. The Epp

of 304 stainless steel was more positive as compared to the pitting potential of the steel in low-concentration solutions.

It is evident from Table 4 that, in the SG solution containing $CaCl_2$, the current density was 1.72×10^{-6} A·cm^{-2} and the Epp was around 0.5 V. In the SG solutions containing Na_2CO_3 and Na_2SiO_3, a larger passivation region led to a more positive Epp. Corrosion products only existed in pitting pits at different concentrations of $CaCl_2$ (Figure 2); thus, the corrosion resistance of the steel was the same in different SG solutions. When different concentrations of Na_2CO_3/Na_2SiO_3 were added, corrosion products accumulated in a layer (Figure 2), increasing the corrosion resistance of the steel in the solutions.

Table 4. Electrochemical parameters obtained from the fitted curves.

40 °C	mM / i/E_{pp}	0	1	5	10	20
$CaCl_2$	i/A·cm^{-2}	1.72×10^{-6}	2.67×10^{-6}	1.91×10^{-6}	1.36×10^{-6}	1.66×10^{-6}
	Epp/V	0.545	0.498	0.524	0.400	0.487
Na_2CO_3	i/A·cm^{-2}	1.72×10^{-6}	3.03×10^{-6}	2.74×10^{-6}	2.37×10^{-6}	2.46×10^{-6}
	Epp/V	0.545	0.528	0.645	0.703	0.969
Na_2SiO_3	i/A·cm^{-2}	1.72×10^{-6}	1.98×10^{-6}	2.11×10^{-6}	2.67×10^{-6}	2.77×10^{-6}
	Epp/V	0.545	0.572	0.988	0.981	0.908

3.2. Characterization of Corrosion Products and the Passivation Film

In order to analyze the morphology and composition of the corrosion products and passivation film, SEM/EDS measurements were performed on the surface of 304 stainless steel treated by polarization measurement in SG, SG + 20 mmol/L $CaCl_2$, SG + 20 mmol/L Na_2CO_3, and SG + 20 mmol/L Na_2SiO_3 solutions.

It is clear from Figure 2 that the nontreated sample surface did not have any corrosion products and pits. In the SG solution, the presence of a small number of granular corrosion products was found near the pit. In the SG + 20 mmol/L $CaCl_2$ solution, granular corrosion products only existed in pits. In the SG + 20 mmol/L Na_2CO_3 solution, the number of granular corrosion products increased greatly, and they existed as clusters. In the SG + 20 mmol/L Na_2SiO_3 solution, the number of corrosion products dramatically increased, and they existed as agglomerates, forming a thin corrosion product layer. Corrosion products generated by the reaction of CO_3^{2-}/SiO_3^{2-} with the steel formed a dense passivation film on the steel surface, generating a protective effect on the steel matrix.

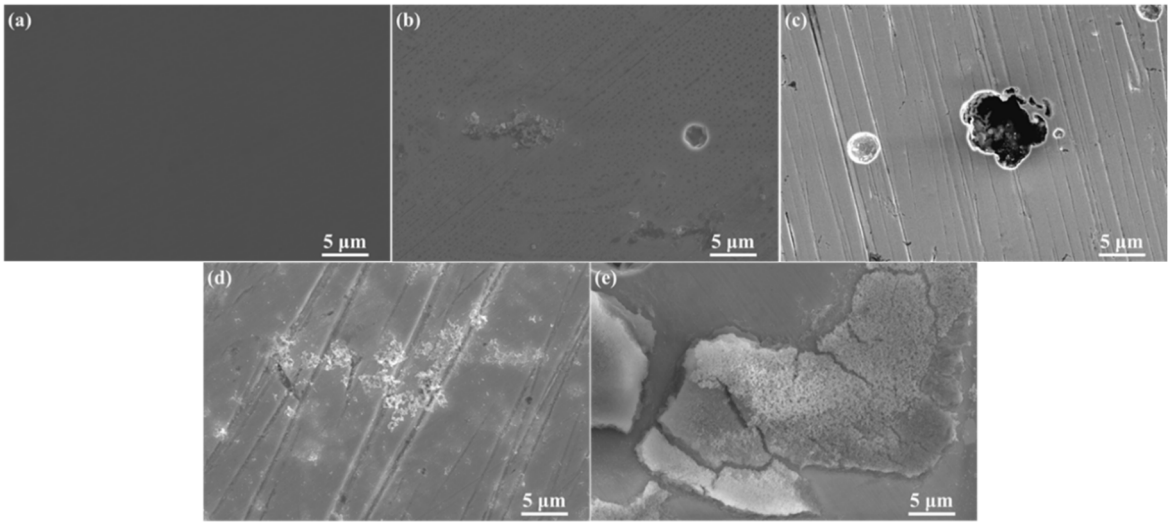

Figure 2. The SEM images of 304 stainless steel treated by polarization measurement in different solutions: (**a**) nontreated; (**b**) SG; (**c**) SG + $CaCl_2$; (**d**) SG + Na_2CO_3; (**e**) SG + Na_2SiO_3.

It is noticeable from Figures 3 and 4 that, after being treated by polarization measurements in the SG solution, corrosion products were mainly composed of Fe and O. After being treated by polarization measurements in the SG + $CaCl_2$ solution, corrosion products generated on the steel surface were mainly composed of Fe, O, and Ca, and they were mainly calcium-rich products and Fe-based compounds, indicating that Ca^{2+} ions were involved in the corrosion reaction. After being treated by polarization measurements in the SG + Na_2CO_3/Na_2SiO_3 solutions, corrosion products were also Fe-based compounds. After the addition of Na_2SiO_3, corrosion products were mainly composed of Fe, O, and Si, indicating that SiO_3^{2-} was involved in the corrosion reaction. Moreover, Fe-based compounds in the corrosion products mainly contained Fe(II) and Fe(III) elements, such as FeO and Fe_3O_4 [2].

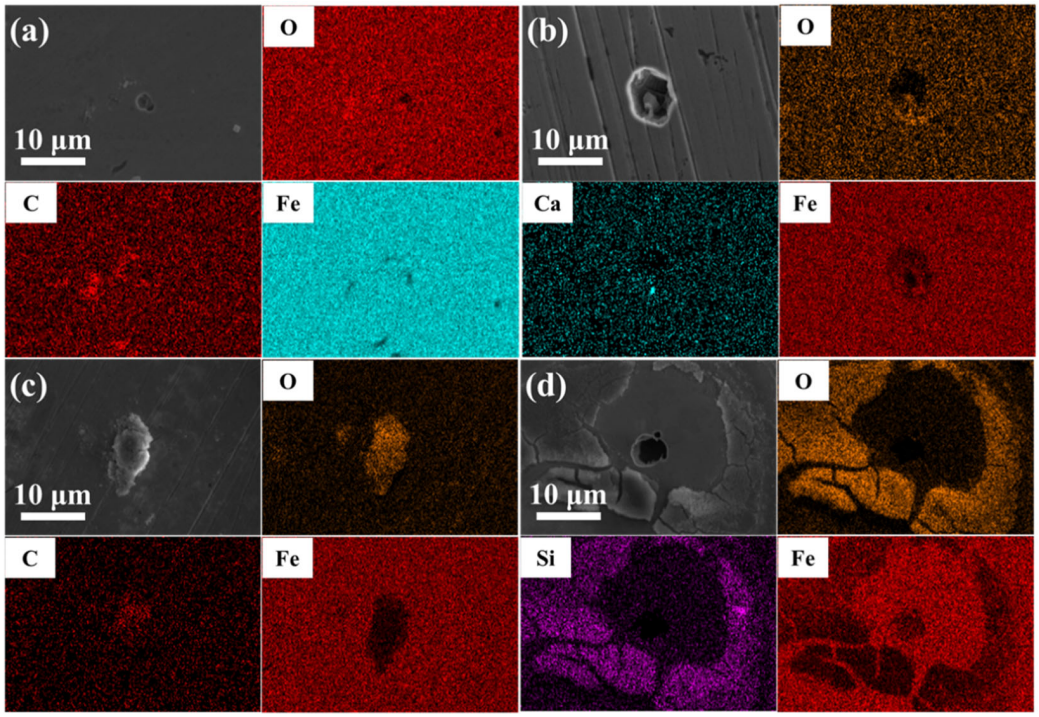

Figure 3. The EDS analysis of 304 stainless steel treated by polarization measurements in different solutions: (**a**) SG; (**b**) SG + $CaCl_2$; (**c**) SG + Na_2CO_3; (**d**) SG + Na_2SiO_3.

Furthermore, the information of products deposited on the surface of 304 stainless steel samples immersed in SG and SG + 20 mmol/L $CaCl_2$/Na_2CO_3/Na_2SiO_3 solutions was obtained by high-resolution XPS spectroscopy, as shown in Figure 5.

The Cr 2*p* spectra in different solutions contained the peaks of Cr_2O_3 (576.1 eV/586.3 eV), CrO_2 (575.4 eV), and $Cr(OH)_3$ (577.4 eV) [16–19] (Figure 5a). Cr in the steel matrix was oxidized to Cr(II/III) compounds and formed a passivation film on the steel surface. The Fe 2*p* spectrum consisted of seven peaks [16–21] (Figure 5b); the peaks of FeOOH (711.8 eV) and Fe_2O_3 (710.8 eV/724.5 eV) were the most significant, while the peaks of FeO (709.8 eV) and Fe_3O_4 (729.5 eV) were relatively weak. The peaks of Fe (706.7 eV/719.9 eV) were the weakest, indicating that Fe in the steel matrix was oxidized to Fe(II/III) compounds and formed a passivation film on the steel surface. In the SG + 20 mmol/L Na_2CO_3 solution, the C 1*s* spectra of corrosion products contained the peaks of C–C (284.4 eV), C–O–C (285.7 eV), and O–C=O (289.1 eV) [21,22] (Figure 5c), indicating the possible presence of CO_3^{2-} ions. In the SG + 20 mmol/L Na_2SiO_3 solution, the Si 2*p* spectra of corrosion products contained the peaks of SiO_2 (102.6 eV) and SiO_3^{2-} (103.7 eV) [22–24] (Figure 5d), indicating that ferric carbonates and silicates were formed after the immersion test.

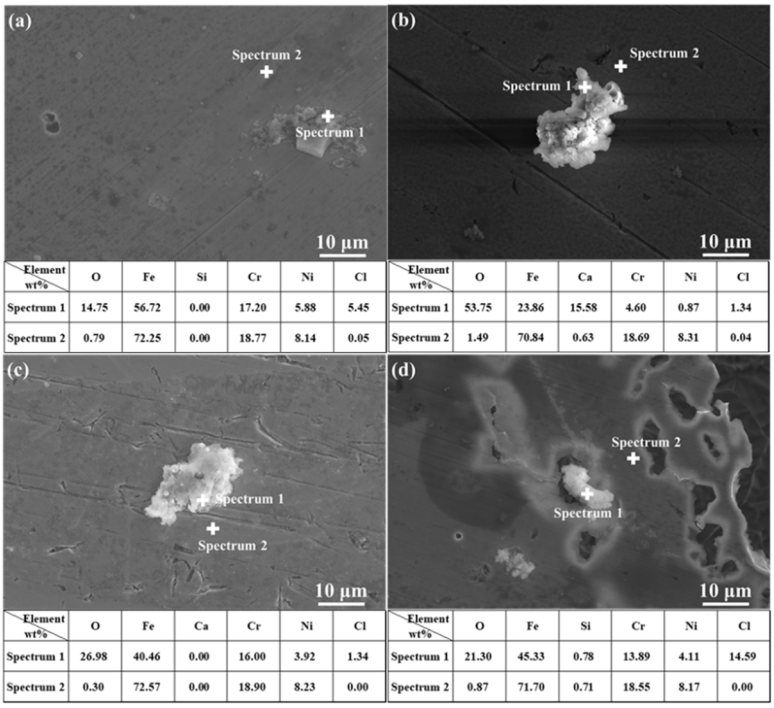

Element wt%	O	Fe	Si	Cr	Ni	Cl
Spectrum 1	14.75	56.72	0.00	17.20	5.88	5.45
Spectrum 2	0.79	72.25	0.00	18.77	8.14	0.05

Element wt%	O	Fe	Ca	Cr	Ni	Cl
Spectrum 1	53.75	23.86	15.58	4.60	0.87	1.34
Spectrum 2	1.49	70.84	0.63	18.69	8.31	0.04

Element wt%	O	Fe	Ca	Cr	Ni	Cl
Spectrum 1	26.98	40.46	0.00	16.00	3.92	1.34
Spectrum 2	0.30	72.57	0.00	18.90	8.23	0.00

Element wt%	O	Fe	Si	Cr	Ni	Cl
Spectrum 1	21.30	45.33	0.78	13.89	4.11	14.59
Spectrum 2	0.87	71.70	0.71	18.55	8.17	0.00

Figure 4. The EDS analysis of 304 stainless steel treated by polarization measurements in different solutions: (**a**) SG; (**b**) SG + $CaCl_2$; (**c**) SG + Na_2CO_3; (**d**) SG + Na_2SiO_3.

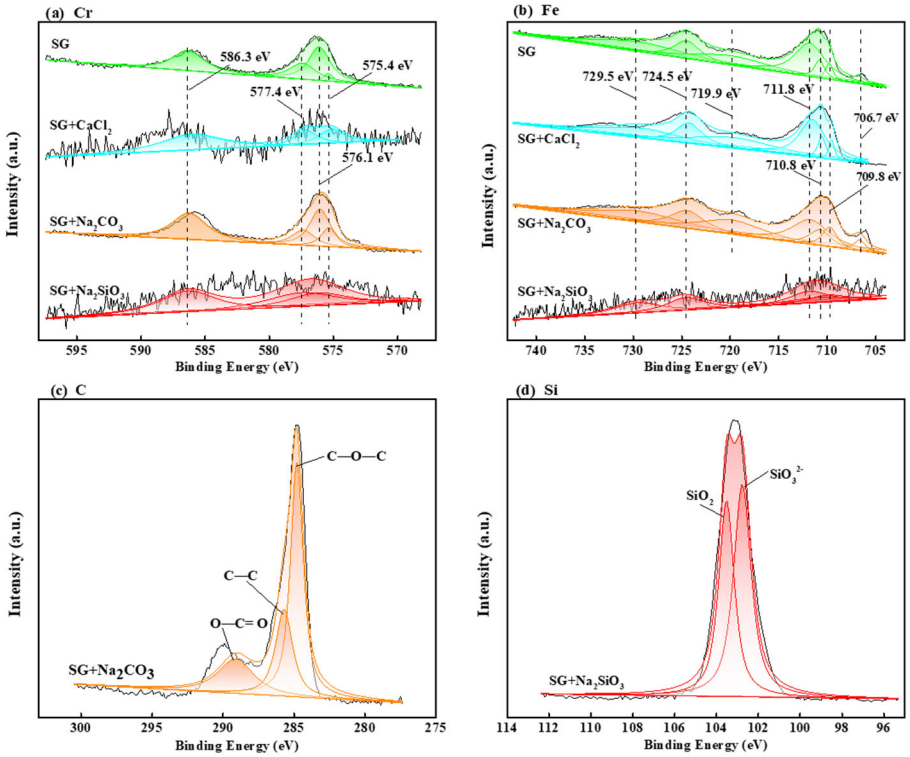

Figure 5. The XPS spectra of 304 stainless steel surfaces obtained after 4 week immersion in SG, SG + 20 mM $CaCl_2$, SG + 20 mM Na_2CO_3, or SG + 20 mM Na_2SiO_3 solutions at 40 °C: (**a**) Cr 2*p*; (**b**) Fe 2*p*; (**c**) C 1*s*; (**d**) Si 2*p*.

From the above experiments and characterization analysis, it can be seen that the Fe(II) compounds produced by the corrosion of 304 stainless steel in SG solutions containing different concentrations of $CaCl_2$, Na_2CO_3, and Na_2SiO_3 were Fe_3O_4, $FeCO_3$, $FeSiO_3$, etc.

3.3. Analysis of the Dissolution Rate of Se after the Immersion Test

The 304 stainless-steel samples treated by polarization measurements were directly immersed in SG + 30 mg/L Na_2SeO_3 solution. It is clear from Figure 6a that the concentration of soluble Se in the solution decreased slightly in the initial stage due to the adsorption effect. As the adsorption effect weakened or disappeared, the amount of dissolved Se in the solution remained negligible during the immersion period. As 304 stainless steel is a self-passivating alloy, the passivation film formed on the surface prevented the steel from reacting with Na_2SeO_3 in the solution; hence, only adsorption reduced the concentration of soluble Se in the solution.

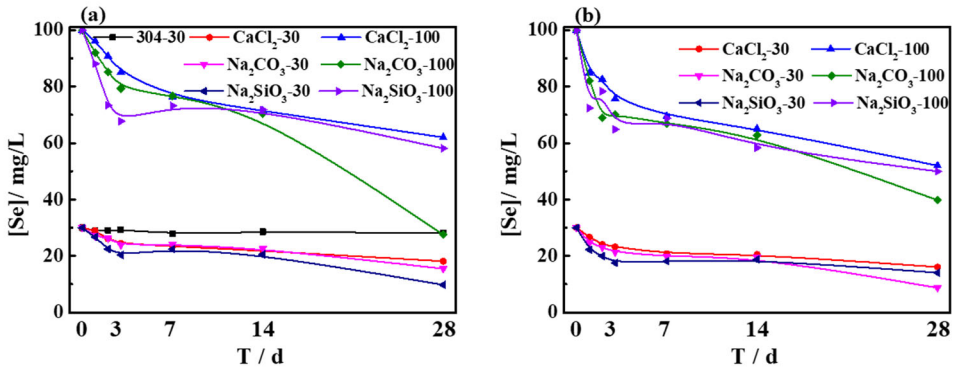

Figure 6. The curve of concentration of dissolved Se plotted against time after treating the 304 stainless steel by polarization measurements in different solutions: (**a**) SG + Na_2SeO_3; (**b**) SG + Na_2SeO_4.

Furthermore, macroscopically, no corrosion products were found on the surface of 304 stainless-steel samples treated by polarization measurements in the SG + 20 mM $CaCl_2$ solution; however, a large number of corrosion products were attached to the steel surface after polarization measurements in the SG + 20 mM Na_2CO_3 and SG + 20 mM Na_2SiO_3 solutions. In addition, a large number of pits and corrosion products existed on the steel surface, as observed by SEM and shown in Figure 2, during polarization measurements. Some of the corrosion products deposited on the steel surface fell off naturally, and the loss of corrosion products in the SG solution containing Na_2SiO_3 was more serious. These samples were subsequently immersed in the solutions in Table 3.

It is observable from Figure 6 that, at the initial stage of immersion, the concentration of soluble Se in the solution decreased rapidly, whereas, at the later stage, the concentration of soluble Se decreased slowly. After treating the steel by polarization measurements in SG + 20 mM Na_2SiO_3 solution, some of the corrosion products fell off naturally, which lowered the reduction rate of soluble Se in the solution of the sample participating in the immersion test. It is clear from Table 5 that the reduction rate of soluble Se was different when the samples were treated by polarization measurements in different solutions. When the samples were treated in the SG solution containing $CaCl_2$, the reduction rates of Se(IV) and Se(VI) were about 40% and 45%, respectively. When the samples were treated in the SG solution containing Na_2CO_3, the reduction rates of Se(IV) and Se(VI) were about 60% and 65%, respectively. When the samples were treated in the SG solution containing Na_2SiO_3, the values were about 50% and 50%, respectively. After polarization measurements, corrosion products were generated on the steel surface and existed in pits. Fe(II) compounds in corrosion products reduced soluble Se(VI) to soluble Se(IV) and then reacted with soluble Se(IV) through a redox reaction. As the samples were adsorbed, the concentration of soluble Se in the solution decreased rapidly in the initial immersion stage. During immersion, the adsorption process weakened, and the presence of the passivation film formed by corrosion products on the surface of the sample weakened the reaction between Fe(II) compounds and Na_2SeO_3, resulting in a slight decrease in the concentration of soluble Se.

Table 5. The soluble Se reduction rate in the immersion test.

	Reduction Rate (%)		
	SG + 20 mM $CaCl_2$	**SG + 20 mM Na_2CO_3**	**SG + 20 mM Na_2SiO_3**
SG + 30mg/L Na_2SeO_3	39.48	48.32	67.36
SG + 100mg/L Na_2SeO_3	37.98	72.46	41.86
SG + 30mg/L Na_2SeO_4	46.28	70.76	53.08
SG + 100mg/L Na_2SeO_4	47.98	60.22	50.02

The above results indicate that the samples treated by polarization measurements in different solutions led to different corrosion conditions on the surface of steel samples. In comparison to the samples not treated by polarization measurements, the treated steel samples could continuously reduce the concentration of soluble Se in the solution, indicating that the concentration of soluble Se in the solution was reduced in two ways: the adsorption process and the redox reaction between Fe(II) compounds in corrosion products and soluble Se. The number of corrosion products greatly affected the reduction of soluble Se.

3.4. Characterization of Corrosion Products after the Immersion Test

The surface morphologies of corrosion products deposited on the surface of 304 stainless steel after the 4 week immersion test in SG + Na_2SeO_3 solutions were similar (Figure 7). Granular corrosion products formed a dense layer and existed as clusters. The corrosion products deposited on the surface of the 304 stainless-steel samples treated by polarization measurement in the SG solution containing $CaCl_2$ were the lowest in number, while the corrosion products deposited on the surface of the 304 stainless-steel samples treated by polarization measurement in the SG solution containing Na_2SiO_3 were the greatest in number.

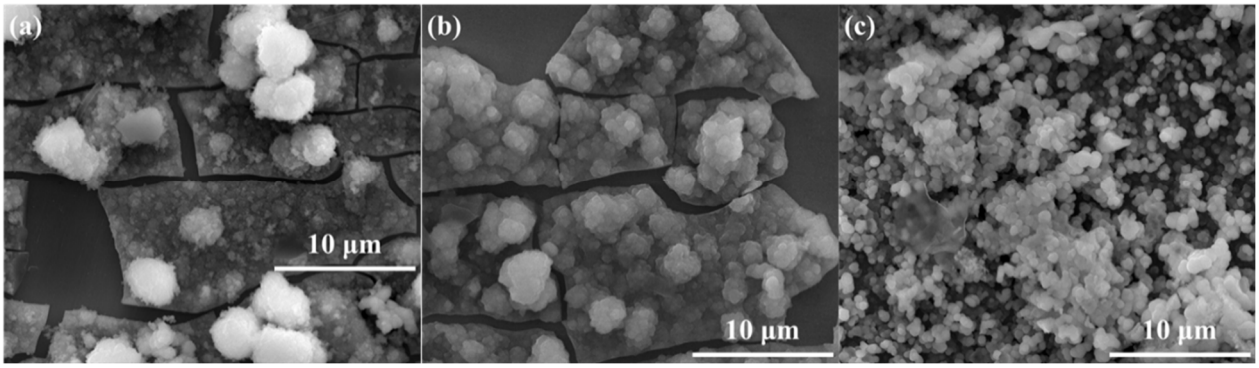

Figure 7. The SEM images of 304 stainless-steel samples after being treated by polarization measurements in different solutions and a 4 week immersion test in SG + Na_2SeO_3 solution: (**a**) SG + $CaCl_2$ solution; (**b**) SG + Na_2CO_3 solution; (**c**) SG + Na_2SiO_3 solution.

It is noticeable from Figures 8 and 9 that the main components of the corrosion products were Fe and Se, indicating that, in the immersion test, Fe(II) compounds in the corrosion products deposited on the treated steel surface were involved in the corrosion reaction. A higher number of corrosion products generated during polarization measurements indicates a greater content of corrosion products generated by Fe–Se compounds on the sample surface during the immersion test. It is preliminarily speculated that the Fe–Se compound was $FeSe_2$.

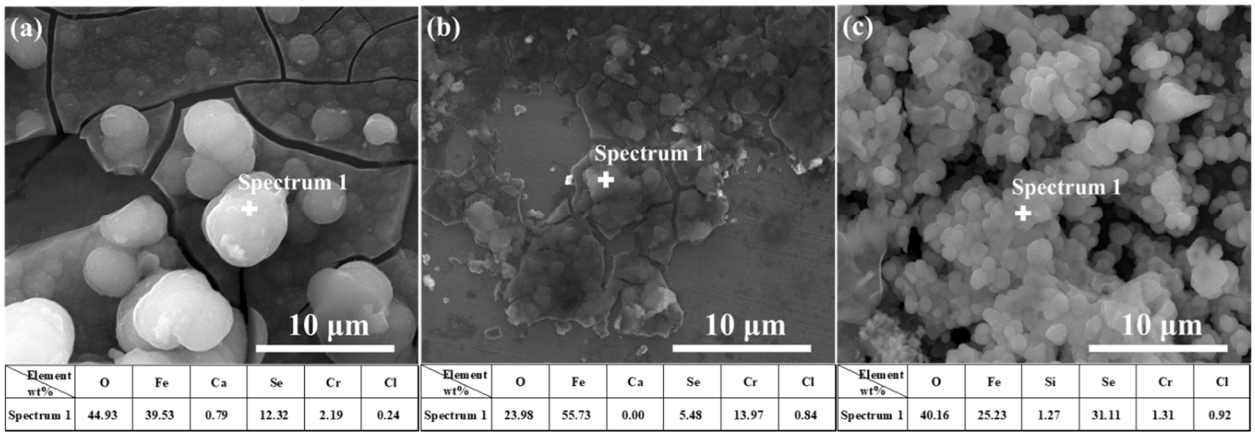

Element wt%	O	Fe	Ca	Se	Cr	Cl
Spectrum 1	44.93	39.53	0.79	12.32	2.19	0.24

Element wt%	O	Fe	Ca	Se	Cr	Cl
Spectrum 1	23.98	55.73	0.00	5.48	13.97	0.84

Element wt%	O	Fe	Si	Se	Cr	Cl
Spectrum 1	40.16	25.23	1.27	31.11	1.31	0.92

Figure 8. The EDS analysis of 304 stainless-steel samples after being treated by polarization measurements in different solutions and a 4 week immersion test in SG + Na_2SeO_3 solution: (**a**) SG + $CaCl_2$ solution; (**b**) SG + Na_2CO_3 solution; (**c**) SG + Na_2SiO_3 solution.

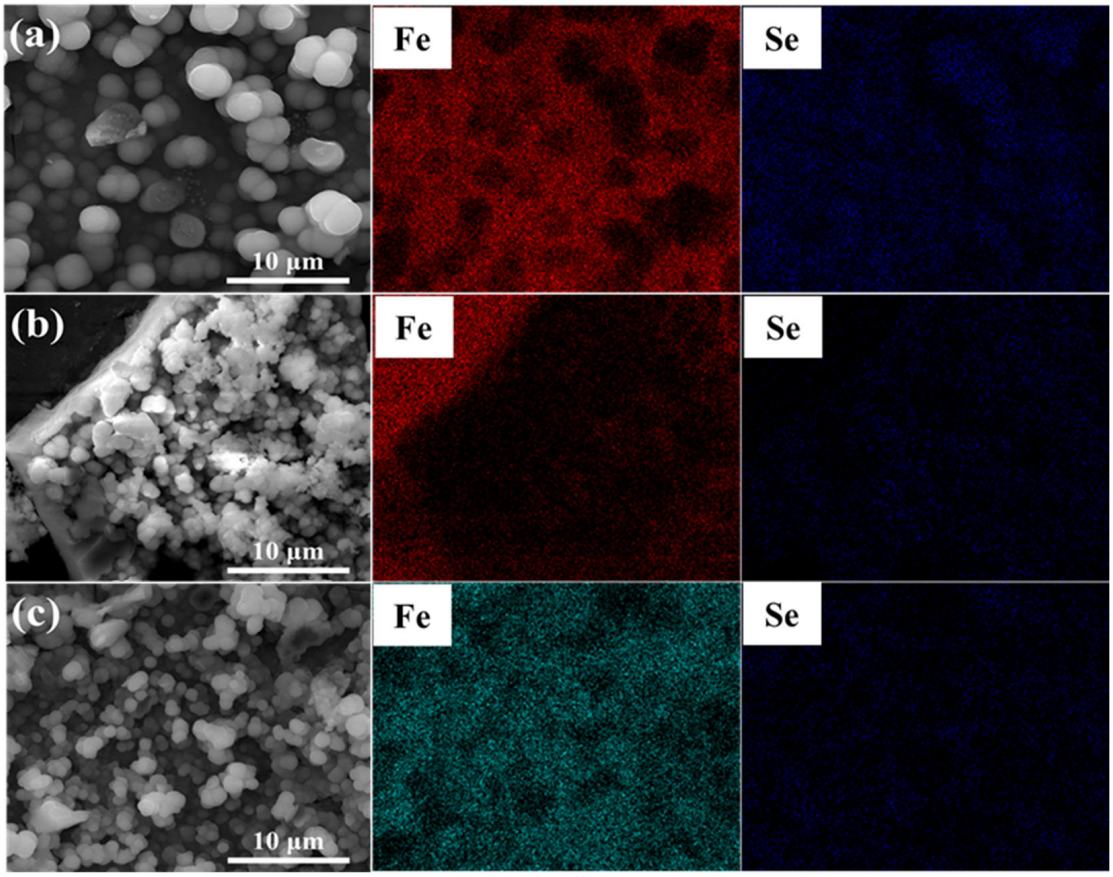

Figure 9. The EDS analysis of 304 stainless-steel samples after being treated by polarization measurements in different solutions and a 4 week immersion test in SG + Na_2SeO_3 solution: (**a**) SG + $CaCl_2$ solution; (**b**) SG + Na_2CO_3 solution; (**c**) SG + Na_2SiO_3 solution.

The surface morphology of corrosion products deposited on the steel surface in the SG + Na_2SeO_4 solution after 4 weeks of immersion was similar to that in the SG + Na_2SeO_3 solution (Figure 10). Corrosion products were granular and existed as agglomerates. The main components of these corrosion products were Fe and Se (Figures 11 and 12).

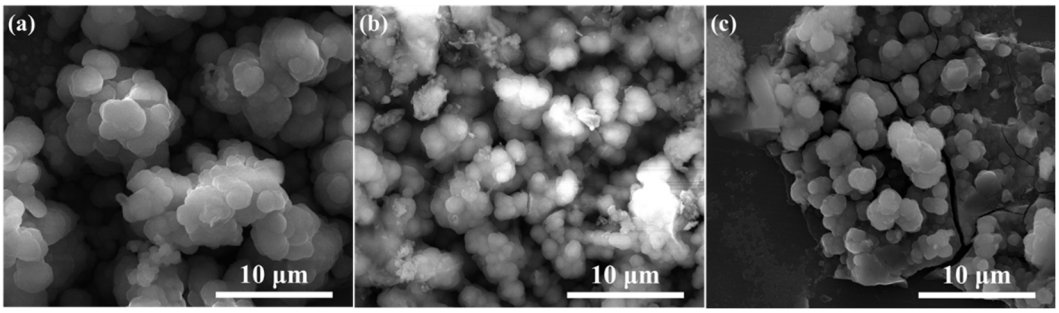

Figure 10. The SEM images of 304 stainless-steel samples after being treated by polarization measurement in different solutions and a 4 week immersion test in SG + Na_2SeO_4 solution: (**a**) SG + $CaCl_2$ solution; (**b**) SG + Na_2CO_3 solution; (**c**) SG + Na_2SiO_3 solution.

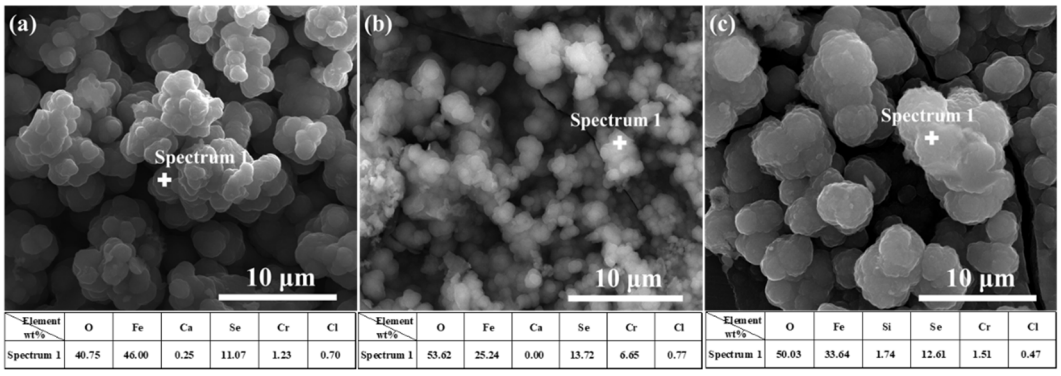

Element wt%	O	Fe	Ca	Se	Cr	Cl
Spectrum 1	40.75	46.00	0.25	11.07	1.23	0.70

Element wt%	O	Fe	Ca	Se	Cr	Cl
Spectrum 1	53.62	25.24	0.00	13.72	6.65	0.77

Element wt%	O	Fe	Si	Se	Cr	Cl
Spectrum 1	50.03	33.64	1.74	12.61	1.51	0.47

Figure 11. The EDS analysis of 304 stainless-steel samples after being treated by polarization measurements in different solutions and a 4 week immersion test in SG + Na_2SeO_4 solution: (**a**) SG + $CaCl_2$ solution; (**b**) SG + Na_2CO_3 solution; (**c**) SG + Na_2SiO_3 solution.

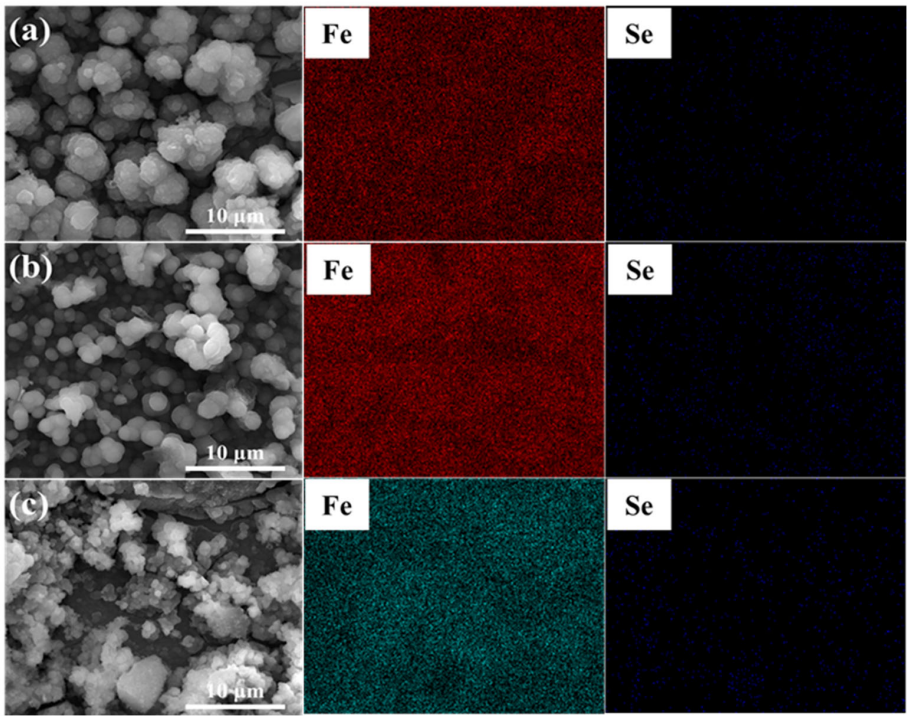

Figure 12. The EDS analysis of 304 stainless-steel samples after being treated by polarization measurements in different solutions and a 4 week immersion test in SG + Na_2SeO_4 solution: (**a**) SG + $CaCl_2$ solution; (**b**) SG + Na_2CO_3 solution; (**c**) SG + Na_2SiO_3 solution.

The Raman spectra of 304 stainless steel after the 4 week immersion test in different solutions are displayed in Figure 13. Corrosion products deposited on the steel surface were mainly composed of Fe–Cr spinel (689 cm^{-1}) and $FeSe_2$ (214 cm^{-1}, 263 cm^{-1}, 212 cm^{-1}, 279 cm^{-1}) [25].

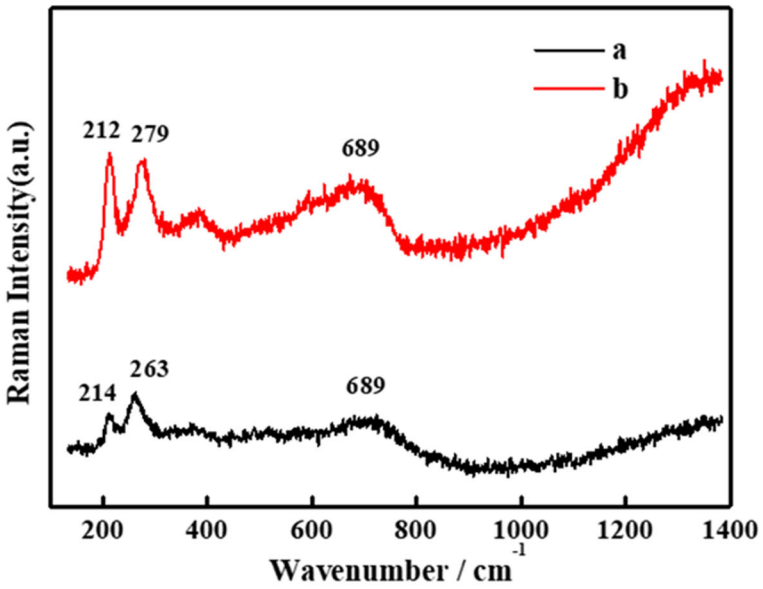

Figure 13. The Raman spectra of 304 stainless-steel samples after a 4 week immersion test in different solutions: (a) SG+ Na_2SeO_3; (b) SG+ Na_2SeO_4.

The above results indicate that corrosion products containing Fe(II) compounds were generated on the 304 stainless-steel surface treated by polarization measurements in SG solutions containing $CaCl_2$, Na_2CO_3, and Na_2SiO_3. Soluble Se(IV) and Se(VI) in the solutions were reduced to $FeSe_2$ by corrosion products. Moreover, a greater number of corrosion products generated during polarization measurements led to a greater content of $FeSe_2$ formed during the immersion test.

3.5. Summary

3.5.1. Corrosion Behavior of 304 Stainless Steel in SG

Pits and corrosion products were generated on the surface of 304 stainless steel samples treated by polarization measurements in SG solutions containing different concentrations of $CaCl_2$, Na_2CO_3, and Na_2SiO_3. In the SG solution containing $CaCl_2$, granular corrosion products only existed in pits. In the SG solutions containing Na_2CO_3 and Na_2SiO_3, granular corrosion products accumulated into layers and increased the corrosion resistance of 304 stainless steel in the solutions. The main corrosion products were Fe_3O_4 and FeO [2,26,27].

Anodic reaction:

$$Fe \rightarrow Fe^{2+} + 2e^{-}. \quad (4)$$

Cathodic reaction:

$$2H_2O + 2e^{-} \rightarrow 2OH^{-} + H_2. \quad (5)$$

Total reaction:

$$Fe + 2H_2O \rightarrow Fe(OH)_2 + H_2, \quad (6)$$

$$Fe^{2+} + {CO_3}^{2-} \rightarrow FeCO_3, \quad (7)$$

$$2Fe^{2+} + {SiO_3}^{2-} + 2OH^{-} \rightarrow Fe_2SiO_4 + H_2O. \quad (8)$$

3.5.2. Effects of Corrosion Products on the Dissolution of Se

Corrosion products deposited on the surface of 304 stainless-steel samples treated by polarization measurements in different SG solutions containing $CaCl_2$, Na_2CO_3, and Na_2SiO_3 contained different amounts of Fe(II) compounds, which reacted with soluble Se to produce $FeSe_2$ during the 4 week immersion test [6].

$$2HSeO_3^- + Fe^{2+} + 10H^+ + 10e^- \rightarrow FeSe_2 + 6H_2O. \quad (9)$$

It was found that Fe(II) compounds could reduce soluble Se at pH = 8.2.

$$SeO_4^{2-} + Fe^{2+} + H^+ \rightarrow Fe^{3+} + SeO_3^{2-} + OH^-, \quad (10)$$

$$2SeO_3^{2-} + Fe^{2+} + 6H^+ + 10e^- \rightarrow FeSe_2 + 6OH^-. \quad (11)$$

A greater number of corrosion products on the surface of 304 stainless steel led to a higher amount of reduced Se in the immersion solutions. The lowest number of corrosion products was deposited on the surface of 304 stainless steel treated by polarization measurements in the SG solution containing $CaCl_2$, and corrosion products only existed in pitting pits. The deposition amount of corrosion products on the surface of 304 stainless steel treated by polarization measurements in the SG solutions containing Na_2CO_3 and Na_2SiO_3 increased. However, during polarization measurements, some corrosion products deposited on the steel surface fell off, and the loss of corrosion products in the SG solution containing Na_2SiO_3 was more serious. The reduction rate R of soluble Se was calculated as $R = 1 - C_1/C_0$, where C_0 is the initial concentration of soluble Se, and C_1 is the final Se concentration after the immersion test; the corresponding results are presented in Table 5.

4. Conclusions

1. Polarization measurements were executed on 304 stainless-steel samples in SG solutions containing $CaCl_2$, Na_2CO_3, and Na_2SiO_3. Corrosion products containing Fe(II) compounds, such as FeO and Fe_3O_4, were generated on the surface of steel samples.
2. The reduction rate of soluble Se was different when the samples were treated by polarization measurements in different solutions. When the samples were treated in the SG solution containing $CaCl_2$, the reduction rates of Se(IV) and Se(VI) were about 40% and 45%, respectively. When the samples were treated in the SG solution containing Na_2CO_3, the reduction rates of Se(IV) and Se(VI) were about 60% and 65%, respectively. When the samples were treated in the SG solution containing Na_2SiO_3, the reduction rates of Se(IV) and Se(VI) were about 50% and 50%, respectively.
3. In Se-containing solutions, Fe(II) compounds in corrosion products reduced soluble Se(VI) to soluble Se(IV), and Fe(II) compounds reacted with soluble Se(IV) through a redox reaction.
4. A large number of corrosion products were generated on the surface of 304 stainless-steel samples treated by polarization measurements. A large amount of $FeSe_2$ was produced on the surface of 304 stainless-steel samples by the 4 week immersion test, and the reduction rate of soluble Se was high.

Author Contributions: G.H. and T.L. wrote the original draft; G.H. prepared all figures; G.H. and T.L. curated data; M.Y. and X.Z. edited the manuscript; M.Y. and X.Z. proposed the conceptualization; L.W. and D.C. managed the project; L.W. and D.C. provided resources. All authors reviewed the manuscript. All authors read and agreed to the published version of the manuscript.

Funding: The financial support from the Nuclear Material Innovation Foundation of China (Grant no. ICNM-2019-ZH-05) is highly acknowledged.

Institutional Review Board Statement: Not applicable.

Informed Consent Statement: Not applicable.

Data Availability Statement: The study did not report any data.

Conflicts of Interest: The authors declare no conflict of interest.

References

1. Björkbacka, Å.; Hosseinpour, S.; Johnson, M.; Leygraf, C.; Jonsson, M. Radiation induced corrosion of copper for spent nuclear fuel storage. *Radiat. Phys. Chem.* **2013**, *92*, 80–86. [CrossRef]
2. Li, T.; Huang, G.; Feng, Y.; Yang, M.; Wang, L.; Cui, D.; Zhang, X. Effects of different ions and temperature on corrosion behavior of pure iron in anoxic simulated groundwater. *Materials* **2020**, *13*, 2713. [CrossRef]
3. Bienvenu, P.; Cassette, P.; Andreoletti, G.; Bé, M.M.; Comte, J.; Lépy, M.C. A new determination of ^{79}Se half-life. *Appl. Radiat. Isot.* **2007**, *65*, 355–364. [CrossRef]
4. Kang, M.; Ma, B.; Bardelli, F.; Chen, F.; Liu, C.; Zheng, Z.; Wu, S.; Charlet, L. Interaction of aqueous Se(IV)/Se(VI) with FeSe/$FeSe_2$: Implication to Se redox process. *J. Hazard. Mater.* **2013**, *248–249*, 20–28. [CrossRef]
5. Kang, M.; Bardelli, F.; Ma, B.; Charlet, L.; Chen, F.; Yang, Y. The influence of pH and reaction time on the formation of $FeSe_2$ upon selenite reduction by nano-sized pyrite-greigite. *Radiochim. Acta* **2016**, *104*, 649–656. [CrossRef]
6. Kang, M.; Chen, F.; Wu, S.; Yang, Y.; Bruggeman, C.; Charlet, L. Effect of pH on aqueous Se(IV) reduction by pyrite. *Environ. Sci. Technol.* **2011**, *45*, 2704–2710. [CrossRef] [PubMed]
7. Myneni, S.C.B.; Tokunaga, T.K. Abiotic selenium redox transformations in the presence of Fe(II,III) oxides. *Science* **1997**, *278*, 1106–1109. [CrossRef]
8. Scheinost, A.C.; Kirsch, R.; Banerjee, D.; Fernandez-Martinez, A.; Zaenker, H.; Funke, H.; Charlet, L. X-ray absorption and photoelectron spectroscopy investigation of selenite reduction by FeII-bearing minerals. *J. Contam. Hydrol.* **2008**, *102*, 228–245. [CrossRef]
9. Scheinost, A.C.; Charlet, L. Selenite reduction by mackinawite, magnetite and siderite: XAS characterization of nanosized redox products. *Environ. Sci. Technol.* **2008**, *42*, 1984–1989. [CrossRef]
10. Han, D.S.; Batchelor, B.; Abdel-Wahab, A. Sorption of selenium(IV) and selenium(VI) to mackinawite (FeS): Effect of contact time, extent of removal, sorption envelopes. *J. Hazard. Mater.* **2011**, *186*, 451–457. [CrossRef]
11. Diener, A.; Neumann, T.; Kramar, U.; Schild, D. Structure of selenium incorporated in pyrite and mackinawite as determined by XAFS analyses. *J. Contam. Hydrol.* **2012**, *133*, 30–39. [CrossRef]
12. Diener, A.; Neumann, T. Synthesis and incorporation of selenide in pyrite and mackinawite. *Radiochim. Acta* **2011**, *99*, 791–798. [CrossRef]
13. Naveau, A.; Monteil-Rivera, F.; Guillon, E.; Dumonceau, J. Interactions of aqueous selenium (-II) and (IV) with metallic sulfide surfaces. *Environ. Sci. Technol.* **2007**, *41*, 5376–5382. [CrossRef]
14. Breynaert, E.; Bruggeman, C.; Maes, A. XANES-EXAFS analysis of se solid-phase reaction products formed upon contacting Se(IV) with FeS_2 and FeS. *Environ. Sci. Technol.* **2008**, *42*, 3595–3601. [CrossRef]
15. Cui, D.; Ranebo, Y.; Low, J.; Rondinella, V.; Spahiu, K. Immobilization of Radionuclides on Iron Canister Material at Simulated Near-field Conditions. In Proceedings of the 2008 MRS Fall Meetin, Boston, MA, USA, 2–4 December 2008.
16. Dou, Y.; Han, S.; Wang, L.; Wang, X.; Cui, Z. Characterization of the passive properties of 254SMO stainless steel in simulated desulfurized flue gas condensates by electrochemical analysis, XPS and ToF-SIMS. *Corros. Sci.* **2020**, *165*, 108405. [CrossRef]
17. Yuan, X.; Wang, X.; Cao, Y.; Yang, H. Natural passivation behavior and its influence on chloride-induced corrosion resistance of stainless steel in simulated concrete pore solution. *J. Mater. Res. Technol.* **2020**, *9*, 12378–12390. [CrossRef]
18. Gardin, E.; Zanna, S.; Seyeux, A.; Allion-Maurer, A.; Marcus, P. Comparative study of the surface oxide films on lean duplex and corresponding single phase stainless steels by XPS and ToF-SIMS. *Corros. Sci.* **2018**, *143*, 403–413. [CrossRef]
19. Dec, W.; Mosiałek, M.; Socha, R.P.; Jaworska-Kik, M.; Simka, W.; Michalska, J. Characterization of Desulfovibrio desulfuricans biofilm on high-alloyed stainless steel: XPS and electrochemical studies. *Mater. Chem. Phys.* **2017**, *195*, 28–39. [CrossRef]
20. Wang, Z.; Feng, Z.; Zhang, L. Effect of high temperature on the corrosion behavior and passive film composition of 316 L stainless steel in high H2S-containing environments. *Corros. Sci.* **2020**, *174*, 108844. [CrossRef]
21. Mayer, T. Black spots on carbon steel after contact to lubricating oil with extreme pressure additives: An XPS study. *Appl. Surf. Sci.* **2001**, *179*, 257–262. [CrossRef]
22. Fang, L.; Liu, Z.; Zhou, C.; Guo, Y.; Yang, M. Degradation Mechanism of Methylene Blue by H_2O_2 and Synthesized Carbon Nanodots/Graphitic Carbon Nitride/Fe(II) Composite. *J. Phys. Chem. C* **2019**, *123*, 26921–26931. [CrossRef]
23. Lopez-Garrity, O.; Frankel, G.S. Corrosion Inhibition of AA2024-T3 By Sodium Silicate. *Electrochim. Acta* **2014**, *130*, 9–21. [CrossRef]
24. De Oliveira, L.A.; Correa, O.V.; dos Santos, D.J.; Páez, A.A.Z.; de Oliveira, M.C.L.; Antunes, R.A. Effect of silicate-based films on the corrosion behavior of the API 5L X80 pipeline steel. *Corros. Sci.* **2018**, *139*, 21–34. [CrossRef]
25. Zheng, Q.; Cheng, X.; Li, H. Microwave synthesis of high activity $FeSe_2$/C catalyst toward oxygen reduction reaction. *Catalysts* **2015**, *5*, 1079–1091. [CrossRef]
26. Thompson, S.P.; Day, S.J.; Parker, J.E.; Evans, A.; Tang, C.C. Fine-grained amorphous calcium silicate $CaSiO_3$ from vacuum dried sol-gel-Production, characterisation and thermal behaviour. *J. Non. Cryst. Solids* **2012**, *358*, 885–892. [CrossRef]
27. Xu, Q.; Gao, K.; Lv, W.; Pang, X. Effects of alloyed Cr and Cu on the corrosion behavior of low-alloy steel in a simulated groundwater solution. *Corros. Sci.* **2016**, *102*, 114–124. [CrossRef]